

A comparing study of quantitative staining techniques for retinal neovascularization in a mouse model of oxygen-induced retinopathy

Xiao-Ling Liang¹, Jie Li^{1,2}, Fang Chen¹, Xiao-Yan Ding¹, Xiu-Xia Yang¹, Liao-Xu Long³

Foundation item: Supported by National Natural Science Foundation of China (No. 30973899)

¹Key Lab of Ophthal Ministry of Edu, Zhongshan Ophthalmic Center, Sun Yat-sen University, Guangzhou 510060, Guangdong Province, China

²Department of Ophthalmology, Nanhai Hospital, Southern Medical University, Foshan 510515, Guangdong Province, China

³Guangzhou Medical University, 195#, Dongfeng Xi Road, Guangzhou, Guangdong Province, China

Correspondence to: Xiao-Ling Liang. Key Lab of Ophthal Ministry of Edu, Zhongshan Ophthalmic Center, Sun Yat-sen University, Guangzhou 510060, Guangdong Province, China. liangxls@yaho.com.cn

Received: 2011-11-05 Accepted: 2012-01-10

Abstract

- **AIM:** To explore an efficient, practical and objective quantitative method to evaluate the retinal neovascularization in mouse model of oxygen induced retinopathy (OIR).
- **METHODS:** Thirty C57BL/6J mice were explored in OIR model procedure. Eyes were removed for different staining methods including: (1) HE staining; (2) immunohistochemistry with Griffonia Simplicifolia Lectin (GSL); (3) Immunofluorescence with FITC labeled CD31 antibody; (4) Two-step immunofluorescence with purified-CD31 antibody; (5) FITC-Dextran perfusion combined with two-step purified-CD31immunofluorescence. Images of the retinal vasculature were analyzed by imaging software.
- **RESULTS:** GSL immunohistochemistry could clearly demonstrate the deep and superficial capillary beds. FITC labeled CD31 Immunofluorescence was blurring with high fluorescence background which was hard to distinguish retinal neovascularization in some area. Excellent detail of neovascularization and preexistent retinal vessels was provided in two-step Purified-CD31 immunofluorescence group.
- **CONCLUSION:** GSL immunohistochemistry can clearly demonstrate neovascularization tufts in deep and superficial capillary beds. Immunofluorescence of specific antigen CD31 on vascular endothelium can selectively label the neovascularization of mouse retina. When combined with

computer analysis software, it is an effective and objective quantitative method to evaluate the retinal neovascularization in OIR mouse model.

- **KEYWORDS:** neovascularization; endothelial cell; CD31, hematoxylin-eosin staining; immunohistochemistry; immunofluorescence; retinopathy of prematurity
- DOI:10.3980/j.issn.2222-3959.2012.01.01

Liang XL, Li J, Chen F, Ding XY, Yang XX. A comparing study of quantitative staining techniques for retinal neovascularization in a mouse model of oxygen-induced retinopathy. *Int J Ophthalmol* 2012; 5(1):1-6

INTRODUCTION

Mouse model of the oxygen-induced retinopathy (OIR)^[1,2] well simulates human proliferative retinopathy in the mechanism and clinical manifestations and the neovascularization is the typical characteristic in this process. Presently, OIR mouse models are widely used in the retinal neovascularization research globally^[3,4,5]. This model is simple, time-saving, well reproducible, cheap as well as source-convenient. To assess and quantify neovascularization in OIR models objectively and rapidly is very important. Previously published methods such as scoring, counting the cell nuclei anterior to the inner limiting membrane and FITC-Dextran perfusion of retinal vessel have some disadvantages such as shortage in quantitative standards, subjectivity, time-consuming or relying on expensive equipment with intricate analysis system^[6-8].

Compared with multiple indices, this study utilizes the agglutinin which showed a high affinity to vascular endothelial cells and the CD31 antibody to label endothelial cells selectively in the retina of mice. We provided an efficient, practical and objective method to quantify neovascularization retinopathy in OIR mouse model.

MATERIALS AND METHODS

Materials Major reagents included Griffonia Simplicifolia Lectin (GSL, Vector Laboratories, USA); Rat anti-mouse CD31 (Purified-CD31), FITC labeled rat anti-mouse CD31 (FITC-CD31) antibody (BD Pharmingen™, USA); Alexa Fluor® 594-labeled goat anti-rat IgG (H+L) (Invivogen,

USA); FITC-Dextran (the molecular weight of 1×10^6 , Sigma, USA); Hydrosoluble Mounting Media (Boster, Wuhan); Optimal cutting temperature (OCT Sakura, USA). Major apparatus included the automatic oxygen controller (BioSperix, USA), Fluorescence microscope and Freezing microtome (Leica, German) as well as light microscope (Olympus, Japan) and micro-syringe (Hamilton, USA).

Animal source: SPF C57BL/6 mice were provided by the Experiment Animal Center of Sun Yat-sen University. Our research adhered to the tenets of the Declaration of Helsinki or the ARVO Statement for the use of Animals in Ophthalmic and Vision Research.

Methods

2.1 OIR mouse model According to the method reported in literatures^[9], postnatal day (P)7 C57BL/6 mice and their maternal mice were exposed to 75% +/- 3% oxygen for 5 days (P7-P11) and then returned to room air for 5 days (P12-P17) for further treatment.

2.2 Grouping Totally 30 mice, 28 of them underwent procedure [2.1] and divided into five groups: 5 mice in the first four groups and 8 mice in the fifth group. Other 2 mice were included as the normal control. All animals were sacrificed on P17 and eyes were collected respectively for procedure [2.3] (Group 1), procedure [2.4] (Group 2), procedure [2.6] (Group 3), procedure [2.7] (Group 4) and procedure [2.8] (Group 5). The normal mouse eye underwent procedure [2.3] and [2.4] only.

2.3 Hematoxylin–Eosin (HE) staining P17 eyeballs were fixed in the formaldehyde-mixing fixative for 24 hours, rehydrated and embedded with paraffin. Serial $6 \mu\text{m}$ sections of whole eyes were cut sagittally through the corneal parallel to the optic nerve. Results were observed under the microscope.

2.4 Frozen section and immunohistochemistry staining with GSL Eyes were embedded with OCT and serial $8 \mu\text{m}$ of section were produced. Sections were fixed with 4% paraffin for 30 minutes, rinsed with 0.05mol/L TBS containing 0.1% Triton for 5min and incubated in the methanol solution containing 30% hydrogen peroxide (1:40) for 20 minutes. 0.05 MTBS containing 10% fetal bovine serum was added to mount at room temperature for 30min and then GSL (1:100) was added at 37°C for 90 minutes. Then, rinsing was repeated. Sections were incubated with peroxidase-avidin for 30 minutes. Then, they were washed for 3 minutes (three times). Some were stained with diaminobenzidine (DAB) and other with eosin as the controls. Sections were observed with a microscope^[10].

2.5 FITC –Dextran heart perfusion and retinal preparation Mice at P17 were anesthetized with 2.5% chloral hydrate and four limbs were fixed. The abdominal cavity was opened. The abdominal aorta was clamped upper the superior border of the liver with a hemostatic forceps.

The diaphragma was split to expose the heart. The right auricle was opened. One miter of 50mg/mL fluorescein-labeled glucose was injected into the left ventricle quickly. The heart perfusion was successful if the heart enlarged and the tongue apex and limbs became yellow. Eyeballs were collected and placed in 10% formaldehyde for half an hour to fix. The cornea, iris and lens were removed. The intact retina was carefully stripped and then was radically incised from the ora serrata along ambituses in four quadrants. Next, the retina was lie down on the slide, which was subsequently mounted with the hydrosoluble mounting medium. Results were observed by fluorescence microscopy.

2.6 One–step immunofluorescence with rat anti–mouse FITC –CD31 antibody Rat anti-FITC-CD31 antibody ($1 \mu\text{L}$) was injected into mice vitreous with a micro syringe on later P16. The needle was inserted vertically at the midpoint of the line connecting the sclera limbus and ambitus. In the next day (P17), eyeballs were collected and placed in 10% formaldehyde for 1-2 hour to fix. The cornea was removed. The lens was taken out to carefully strip the intact retina followed by retinal preparation. The resulting retina was mounted with the hydrosoluble mounting medium.

2.7 Two–step immunofluorescence with rat anti–mouse Purified –CD31 antibody Eyeballs of fresh mice were collected and then fixed for 1-2 hour in 10% formaldehyde. The cornea was removed. The crystal was taken out and then the intact retina was carefully stripped. Retinal tissues were washed with PPS 20min \times 4 and then soaked with PBST-BSA (0.5%Triton-X100+3%BSA) at room temperature for 1 hour or at 4°C overnight. PBST-BSA was removed. The primary antibodies (rat anti-mouse CD31 antibodies (1:25)) were added for 2 hours at room temperature followed by standing 4°C overnight. Then, washing with PBST 20min \times 4 was repeated. After that, secondary antibodies (Alexa Fluor[®] 594 goat anti-rat antibodies (1:100)) were added to incubate for 1 hour at 37°C (keeping away from light). Then, retinas were washed with PBST repeatedly. The resulting retina was mounted with the hydrosoluble mounting medium.

2.8 FITC–Dextran heart perfusion in combination with two –step immunofluorescence with rat anti –mouse Purified CD31 antibody Procedures were shown in sections 2.5 and 2.7.

Statistical Analysis Image Pro[®] Plus image analysis software was used to process, analyze and measure the neovascularization. SPSS v.17.0 was applied for statistical analysis. Results of CD31 labeled method and FITC perfusion method were compared by univariate ANOVA. $P < 0.05$ was considered as significant.

RESULTS

Comparison of Paraffin Section HE Staining and Frozen Section GSL Immunohistochemical Staining Both

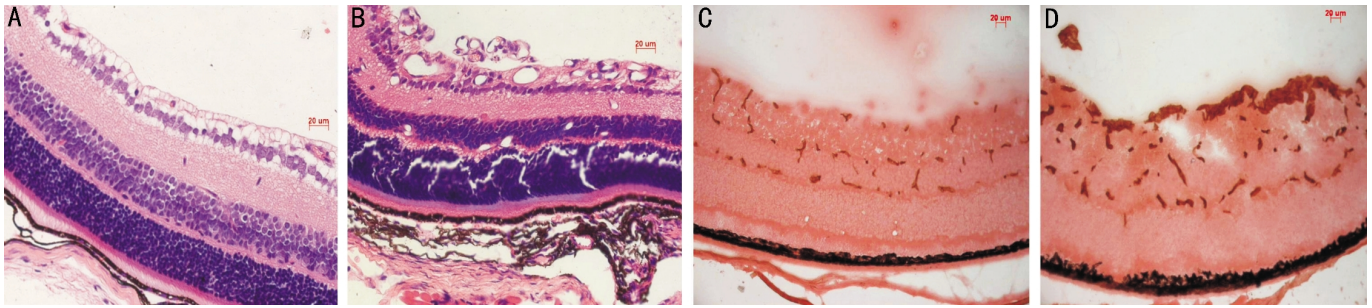


Figure 1 Comparison of paraffin section HE staining and frozen section GSL immunohistochemical staining of OIR mouse retina A,C: normal retina; B,D: OIR mouse retina. Both HE (B) and GSL (D) staining showed a disorder of retinal layers and considerable neovascularization in OIR mouse retina. GSL staining could clearly display the neovascular tissues penetrated the inner limiting membrane and those in deep vessel bed. Pathological neovascular could be easy distinguished from surrounding tissues.

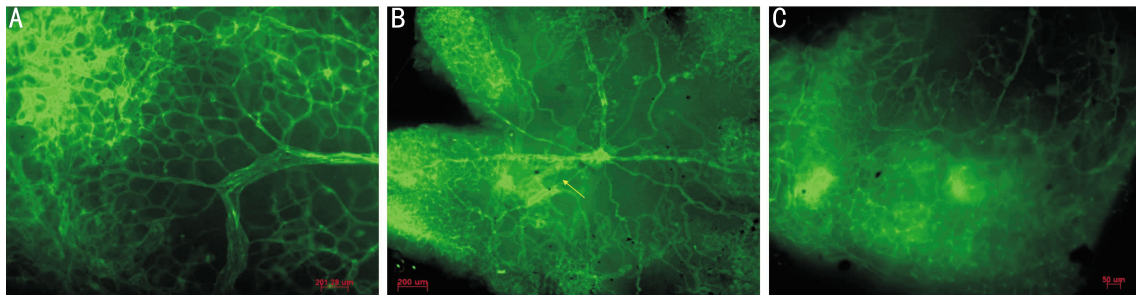


Figure 2 One-step immunofluorescence with rat anti-mouse FITC-CD31 antibody A: Intravitreal injection of FITC-labeled rat anti-mouse CD31 *in vivo* could label superficial and deep retinal vessels in OIR mice; B: Residuary hyaloid artery was seen in a few of retinas (arrow); C: High fluorescent background and suspected remnant vitreous made it hard to further analyze quantify this image.

HE and GSL staining showed a disorder of retinal layers and considerable neovascularization in OIR mouse retina. Due to selectivity to endothelial cells, GSL staining could clearly display the neovascular tissues penetrated the inner limiting membrane and neovascularization in superficial or deep vessel bed. Pathological neovascular could be easy distinguished from surrounding tissues. Image Pro® Plus image analysis software indicated that GSL staining could objectively, safely and conveniently display neovascular tissues(Figure 1).

One-step Immunofluorescence with Rat Anti-mouse FITC-CD31 Antibodies Results proved that FITC-labeled rat anti-mouse CD31 injected in the vitreous could label vascular tissues in the retina of OIR mice. Images produced by the one-step method could display the normal deep and superficial vessels beds as well as neovascularization. However, the retinas prepared by this method still had a high fluorescent background. Meanwhile, the suspected remnant vitreous affected observation of the retinal neovascularization(Figure 2).

Two-step Immunofluorescence with Rat Anti-mouse Purified -CD31 Antibodies Patchy or flexiform neovascularization were clearly visible in peripheral retina of OIR mice under the low power microscope. The demarcation between posterior avascular area and peripheral capillary bed was distinct. The capillary bed in the deep retina and distorted, enlarged or patchy neovascular tufts on the surface of the retina were clearly observed under the

high power microscope. The residuary hyaloid artery presented in some cases (Figure 3).

FITC-Dextran Heart Perfusion Combined with Two-step CD31 Immunofluorescence The retina was cut into the four-leaved petal-like shape. Utilizing the double-channel function of the fluorescence microscope, different fluorescent signals in the same area of the retina were captured (green: FITC; red: CD31). Two types of signals coincided with each other. Both of them could display neovascularization in the retina clearly. However, in some cases, peripheral retina neovascularization labeled by the FITC perfusion seemed dim with obscure boundary, which increased the subjectivity, error and reliability. Moreover, we could find a considerable filling defect of FITC-Dextran in some peripheral parts of retina and incomplete perfusion in some central retina vessels. However, CD31 immunofluorescence was able to display patchy neovascularization, distorted and expanded retinal vessels clearly as well as the demarcation between central avascular area and peripheral capillary bed. Areas of neovascularization stained with FITC and CD31 immunofluorescence were measured by the Image Pro® Plus analysis software. We used the function named automatic recognition (area of interest: AOI function) of Image Pro® Plus software to avoid bias and subjectivity. The area was $1.31 \pm 0.21 \text{mm}^2$ for CD31 labeling method and $1.11 \pm 0.19 \text{mm}^2$ for FITC-Dextran perfusion method ($P = 0.51 > 0.05$). The correlation of both method was excellent($r = 0.97$, Figure 4,5;Table 1)^[11,12].

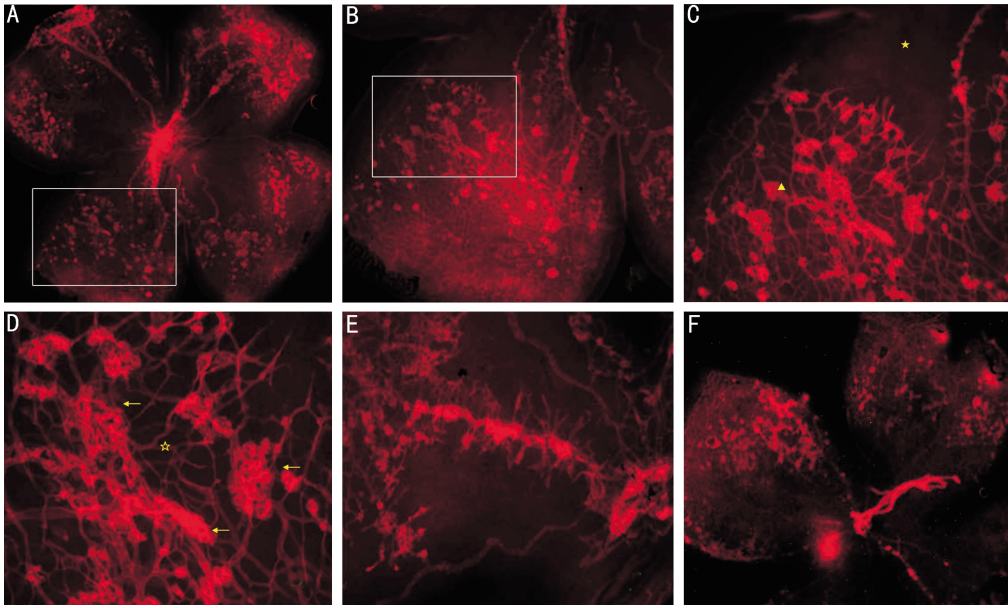


Figure 3 Two-step immunofluorescence with rat anti-mouse Purified-CD31 antibody A, B: Neovascularization in the peripheral retina and avascular area surrounding papilla optica were displayed clearly under low power microscope; C, D: The capillary bed (▲) and avascular area (★) had obvious boundaries. The capillary bed in the deep retina (☆) and the superficial distorted, enlarged or patchy neovascularization plexus (←) were clearly observed under the high power microscope; E: The central retina vessels were distorted, expanded or accompanied with fungus-like angiogenesis; F: The residuary hyaloid artery was labeled in some cases.

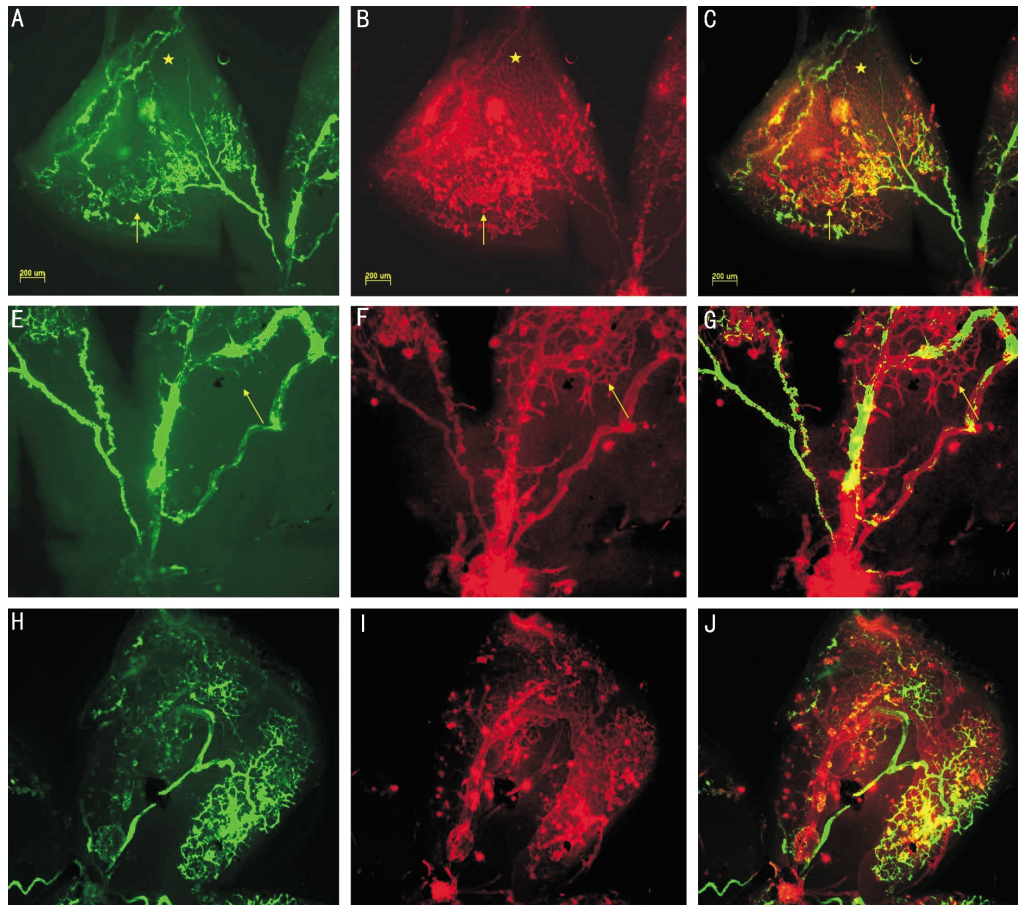


Figure 4 FITC-Dextran heart perfusion combined with two-step CD31 immunofluorescence Green: FITC-Dextran signal; Red: CD31 signal. All figures showed that both FITC-Dextran perfusion and CD31 immunofluorescence methods could label neovascularization in the retina clearly and they could fused together basically. A, B, C: Compared to CD31 immunofluorescence, neovascularization in the left inferior retina labeled by the FITC-Dextran perfusion were dim with an obscure boundary which increased the measurement subjectivity and reliability (arrow). Moreover, considerable capillaries had filling-defect (★); E, F, G: FITC-Dextran filling-defect of central retina vessels caused its small arterial branches as well as capillaries deficiency; H, I, J: CD31 immunofluorescence clearly displayed the patchy, mottled neovascularization and the distorted and expanding central vessels in the retina rather than FITC-Dextran filling deficiency.

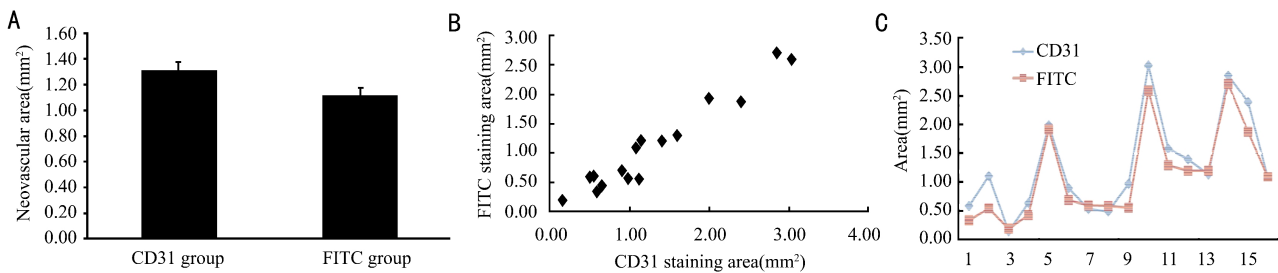


Figure 5 Comparison between FITC –Dextran perfusion and two –step CD31 immunofluorescence in labeling retinal neovascularization A,B: The correlation of the two methods was excellent ($r = 0.97$); C: The area was $1.31 \pm 0.21 \text{mm}^2$ by CD31 immunofluorescence and $1.11 \pm 0.19 \text{mm}^2$ by FITC-Dextran perfusion method. The later one decreased by 15.2%, however, the difference was not statistically significant.

Table 1 Comparison between FITC perfusion and CD31 immunofluorescence in labeling retinal neovascularization area (mm²)

	1	2	3	4	5	6	7	8	9	10	11	12	13	14	15	16	Average
FITC signal	0.34	0.55	0.20	0.43	1.92	0.69	0.60	0.59	0.56	2.59	1.30	1.20	1.20	2.70	1.87	1.09	1.11 ± 0.19
CD31 signal	0.59	1.11	0.16	0.64	1.99	0.90	0.54	0.50	0.98	3.02	1.59	1.40	1.14	2.85	2.39	1.08	1.31 ± 0.21

DISCUSSION

Mouse model of Oxygen-induced retinopathy is widely accepted and used in the study of mechanism, pathophysiology and treatment of retinal neovascularization. It well simulates the development process of the retinal neovascularization. How to assess and quantify the neovascularization of retinopathy objectively, effectively and efficiently is very important^[13].

Previously, there were three main strategies to assess neovascularization of retinopathy in OIR animal model. The first qualitative method involving counting or scoring capillary tufts in FITC-Dextran perfusion retina which seemed similar to the clinical assessment of retinopathy of prematurity (ROP)^[6]. The second method was to count cell nucleus population penetrating the inner limiting membrane^[14] in the HE or PAS ocular sections^[6,7]. The third kinds of method was to quantify the neovascular area or density^[15] and distinguish physical and pathological vessels in the FITC-Dextran perfusion retina by a confocal microscope. Generally, these methods have some disadvantages such as time-consuming, subjective, lacking of quantitative criteria, relying on high-tech or expensive instruments etc.

Due to the widely utilization of the paraffin and frozen section in clinical and basic research, both of them are simple and practicable^[15]. In our study, we used the GSL to bind the surface of endothelial cells, which identified pathological neovascularization clearly in the retina within a short time. With high contrast to the background, we could distinguish and quantify the pathological vessels easily by using image analysis software. When compared with counting nucleus, the GSL staining method is more objective and efficient. Shen *et al*^[6] have reported their research on the physiopathological process of retinal neovascularization proliferation and atrophy by labeling retinal vascular endothelial cell antigen PECAM1 (CD31) and macrophage

surface antigen F4/80. Based on the principle, the study proves that intravitreal injection of FITC-labeled rat anti-mouse CD31 *in vivo* can fully label retinal vessels. However, high background fluorescence and suspected remnant vitreous made it hard to observe vessel structures clearly. Meanwhile, the retina is too crisp to succeed in retinal preparation, which may be related to endophthalmitis or non-specificity inflammation reaction caused by intravitreal injection. It suggest that the direct staining of retinal neovascularization by intravitreal injection FITC-labeled rat anti-mouse CD31 seems not as practicable as tow step staining.

In previous literatures, FITC-Dextran perfusion was a widely used method to quantify the neovascularization in OIR animal retinopathy^[1, 2,17]. However, this widely accepted method seems not perfect anyway. In our study, 16 eyeballs (8 mice) were perfused with FITC-Dextran followed by two-step immunofluorescence with rat anti-mouse Purified-CD31 antibody. The same fluorescence microscope and software were used to quantify the neovascularization of the retina. We found that many CD31-labeled capillary tissues were not labeled by FITC-Dextran perfusion. The possible reasons for FITC perfusion defect may include the following speculation: (1) Circulation function failure. Before perfusion, deep anesthesia, long exposure of the heart or cardiac arrest may cause thrombosis in the retina vessels which blocks complete perfusion. (2) Perfusion techniques. If the needle does not penetrate the left ventricular wall, the perfusion solution can be leaked out through the needle tip; conversely, if the needle penetrates the left ventricle or incarcerates in the myocardium, the perfusion solution could not enter the aorta smoothly. This may causes unstable perfusion pressure which results in intermittent peripheral vessel perfusion. (3) Perfusion solution. Dosage and concentration variation of FITC-Dextran solution may

results in different perfusion. (4) Physical factor. Extreme pH (over low or high) and low temperature of the perfusion solution may induce angiospasm and vasoconstriction. (5) Pathological factor. New vessel is formed in two modes: vasculogenesis and angiogenesis^[17,18]. Neovascularization in proliferative retinopathy primarily is a angiogenesis process, in which, new vessel generate from original vessels^[18,19]. Though proliferation and migration, the endothelia cell break through the basement membrane of vessels and invade peripheral tissues. Then the neovascularization bud form lumina gradually. The vessel lumina formation completed when adjacent neovascularization bud anastomosed and microcirculation formed. In some retinal pathological neovascularization, lumina may not be fully formed or anastomosed. Obviously, these vessels are the "blind area" of perfusion.

In addition, Two types of fluorescent signal (green: FITC; red: CD31) coincided with each other. This suggested that the both methods were acceptable to be used to quantify retinopathy^[21,22]. However, selectively staining the specific antigen CD31 of endothelium can display neovascularization distribution and avascular area in the retina clearly. It has no "blind area" which is present in FITC-Dextran perfusion. It also provided a choice for investigating ophthalmological embryology by staining residuary hyaloid artery. Noticeably, CD31 antigen staining could label retinal neovascularization much more obviously compare to normal vessels. The mechanism is unclear. We speculated that high expression of CD31 or special features of neovascularization increase its affinity to anti-CD31 antibodies. High-contrast between neovascularization and normal vessels combined with automatic recognition (area of interest: AOI function) of Image Pro[®] Plus software could increase the quantitative objectivity and efficiency dramatically.

In conclusion, frozen section for GSL staining can clearly demonstrate neovascularization tufts in deep and superficial capillary beds on OIR mouse retina. Labeling specific antigen CD31 on vascular endothelium by Immunofluorescence can stain the retinal neovascularization selectively. Moreover, when combined with computer analysis software, it is an efficient, practical and objective quantitative method to evaluate the retinal neovascularization in OIR mouse model.

REFERENCES

- 1 Smith LE, Wesolowski E, McLellan A, Kostyk SK, D'Amato R, Sullivan R, D'Amore PA. Oxygen-Induced Retinopathy in the Mouse. *Invest Ophthalmol Vis Sci* 1994;35:101-111
- 2 Ding XY, Li T, Xie SZ, Ma HJ, Li B, Tang SB. The temporal and spatial Norrin expression and significance in oxygen induced retinopathy. *Zhongguo Bingli Shengli Zazhi* 2008;24(3):543-547
- 3 Zhao M, Shi X, Liang J, Miao Y, Xie W, Zhang Y, Li X. Expression of pro- and anti-angiogenic isoforms of VEGF in the mouse model of oxygen-induced retinopathy. *Exp Eye Res* 2011;93(6):921-926
- 4 Bromberg-White JL, Boguslawski E, Hekman D, Kort E, Duesbery NS. Persistent inhibition of oxygen-induced retinal neovascularization by anthrax lethal toxin. *Invest Ophthalmol Vis Sci* 2011;52(12):8979-8992
- 5 Jhanji V, Liu H, Law K, Lee VY, Huang SF, Pang CP, Yam GH. Isoliquiritigenin from licorice root suppressed neovascularisation in experimental ocular angiogenesis models. *Br J Ophthalmol* 2011;95 (9): 1309-1315
- 6 Chikaraishi Y, Shimazawa M, Hara H. New quantitative analysis, using high-resolution images, of oxygen-induced retinal neovascularization in mice. *Experimental Eye Research* 2007;84: 529-536
- 7 Sharma J, Barr SM, Geng Y, Yun Y, Higgins RD. Ibuprofen improves oxygen-induced retinopathy in a mouse model. *Curr Eye Res* 2003;27 (5): 309-314
- 8 Elner SG, Elner VM, Yoshida A, Dick RD, Brewer GJ. Effects of tetrathiomolybdate in a mouse model of retinal neovascularization. *Invest Ophthalmol Vis Sci* 2005;46(1): 299-303.
- 9 Liang XL, Huang YS, Chen HY, Guo XH, Yu SS, Xie SZ, Yan J, Tang SB. Inhibition of gene expression of VEGF, PECAM and neovascularization of retina by cyclic Heptadepsipeptide. *Zhongshan Daxue Xuebao* 2005: 26(6):607-611,621
- 10 Ding XY, Liang XL, Xie SZ, Zhu Xiaobo, Tang SB. A Modified Mouse Model of Oxygen induced Retinopathy. *Yanke Xuebao* 2006;22:98-102
- 11 McGinley JN, Thompson HJ. Quantitative assessment of mammary gland density in rodents using digital image analysis. *Biol Proced Online* 2011;10;13(1):4
- 12 Jiang JL, Liu WR, Yu YY, Ni PH, Wu JL, Ji J, Zhang JN, Chen XH, Lu BY, Zhu ZG. Establishment of experimental angiogenic models with applications of quantitative digital image analysis. *Zhonghua Binglixue Zazhi* 2011;40(7):475-479
- 13 Grossniklaus HE, Kang SJ, Berglin L. Animal models of choroidal and retinal neovascularization. *Prog Retin Eye Res* 2010;29(6):500-519
- 14 Zhang HR. Clinical and Basic Research on Retinal Diseases. Shan Xi: Shan Xi Science & Technology Publishi House 1995:323
- 15 Al-Shabraway M, El-Remessy A, Gu X, Brooks SS, Hamed MS, Huang P, Caldwell RB. Normal vascular development in mice deficient in endothelial NO synthase: possible role of neuronal NO synthase. *Mol Vis* 2003; 9:549-558
- 16 Shen J, Xie B, Dong A, Swaim M, Hackett SF, Campochiaro PA. In Vivo Immunofluorescence Demonstrates Macrophages Associate with Growing and Regressing Vessels. *Invest Ophthalmol Vis Sci* 2007;48: 4335-4341
- 17 Campochiaro PA. Retinal and Choroidal Neovascularization. *J Cell Physiol* 2000; 184:301-310
- 18 Gerhardt H, Golding M, Fruttiger M, Ruhrberg C, Lundkvist A, Abramsson A, Jeltsch M, Mitchell C, Alitalo K, Shima D, Betsholtz C. VEGF guides angiogenic sprouting utilizing endothelial tip cell filopodia. *J Cell Biol* 2003; 161:1163-1177
- 19 Sapielha P, Joyal JS, Rivera JC, Kermorvant-Duchemin E, Sennlaub F, Hardy P, Lachapelle P, Chemtob S. Retinopathy of prematurity: understanding ischemic retinal vasculopathies at an extreme of life. *J Clin Invest* 2010;120(9):3022-3032
- 20 Sears JE, Hoppe G, Ebrahim Q, Anand-Apte B. Prolyl hydroxylase inhibition during hyperoxia prevents oxygen-induced retinopathy. *Proc Natl Acad Sci* 2008;105(50):19898-19903
- 21 Dimaio TA, Wang S, Huang Q, Scheef EA, Sorenson CM, Sheibani N. Attenuation of retinal vascular development and neovascularization in PECAM-1-deficient mice. *Dev Biol* 2008;315(1):72-88